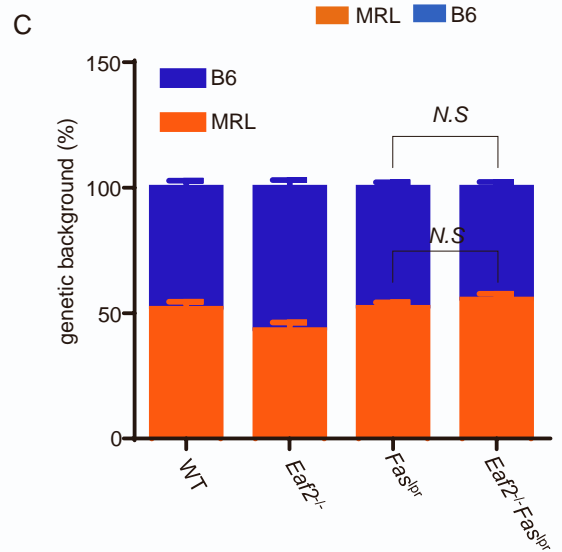
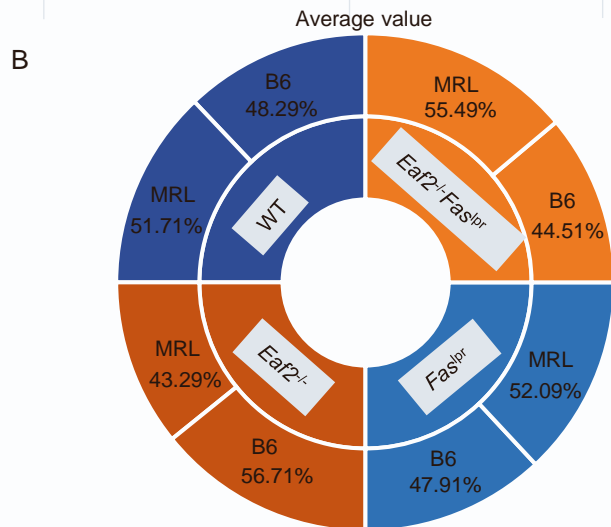
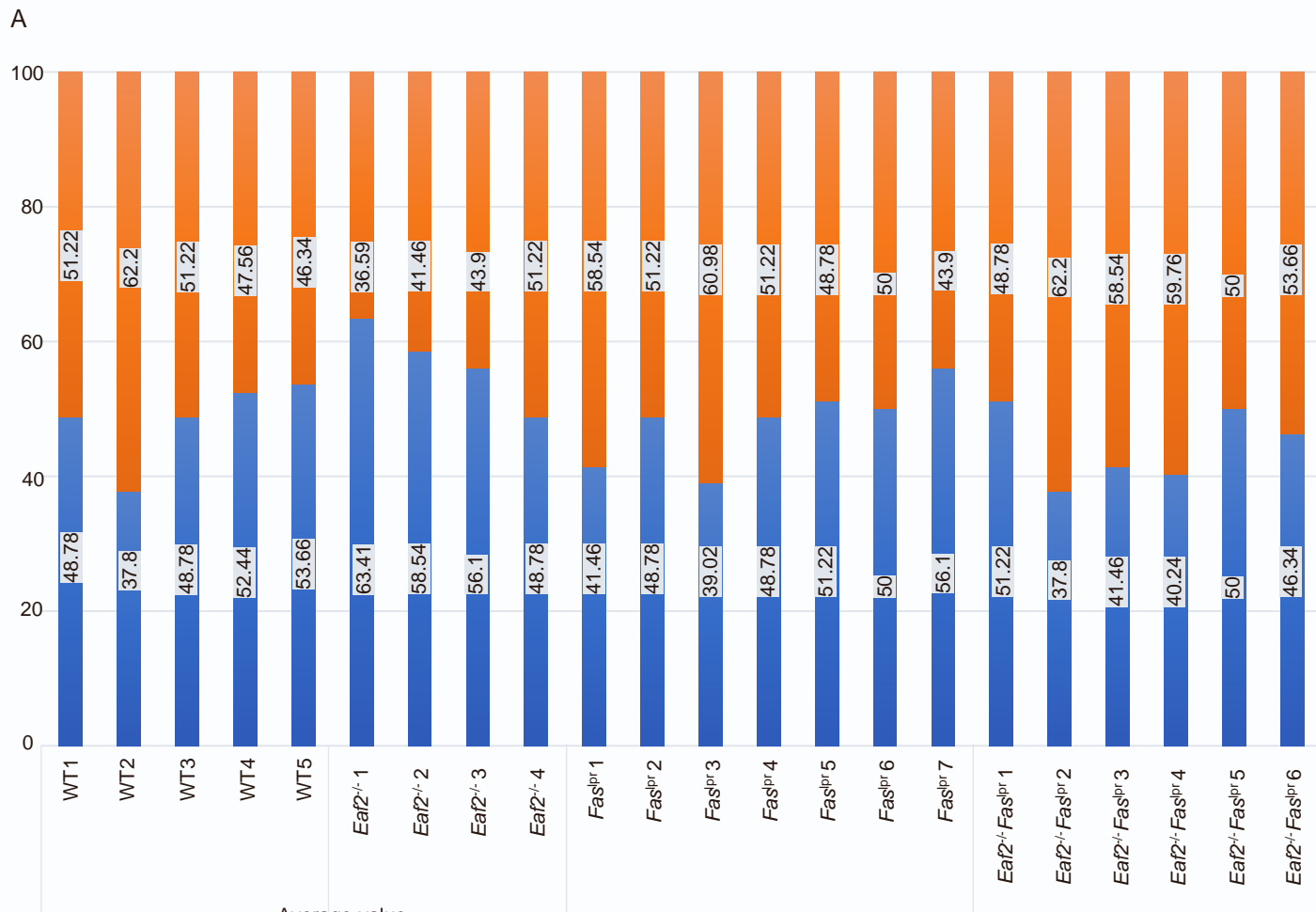


iScience, Volume 27

## Supplemental information

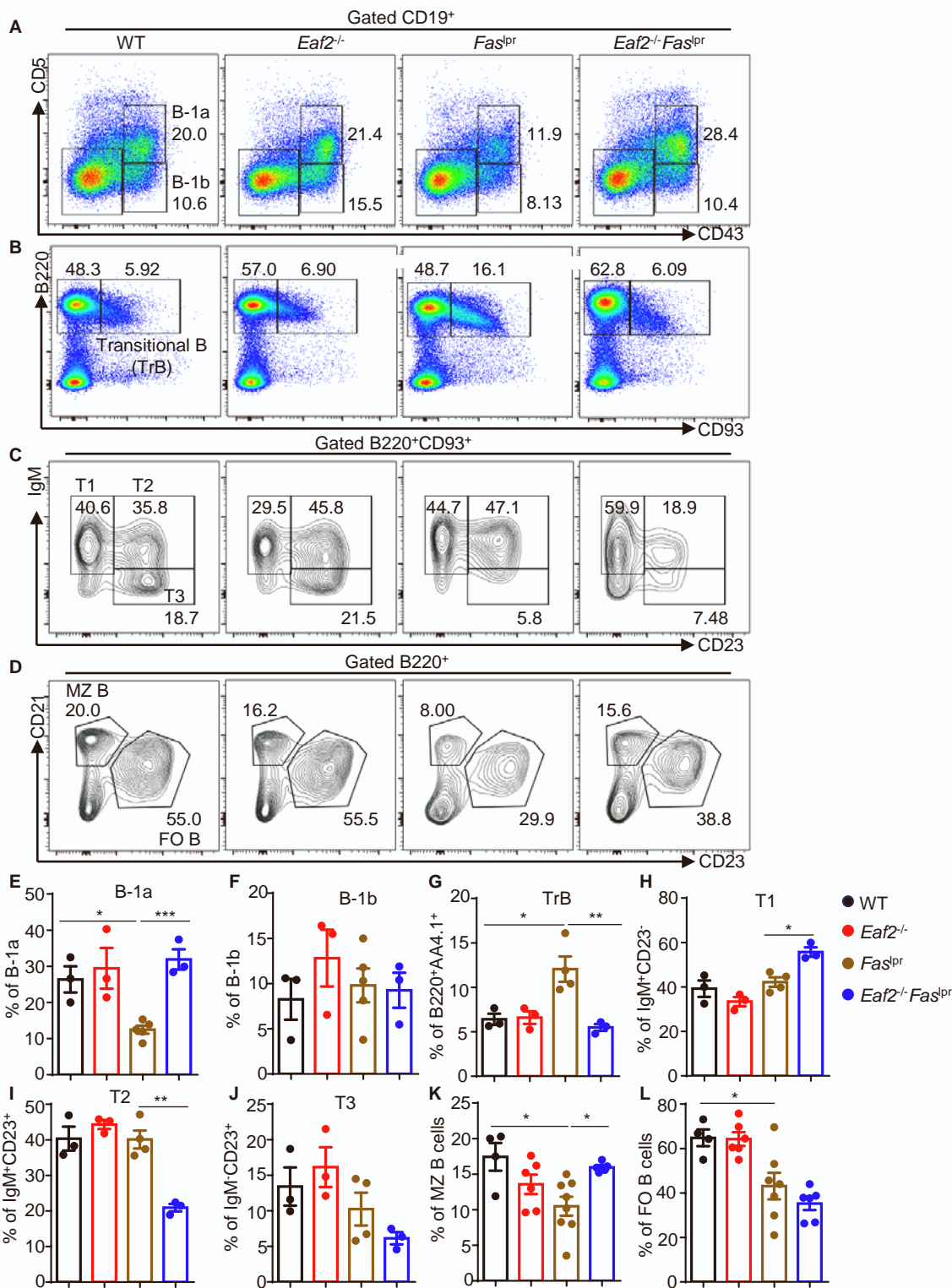
### **EAF2 deficiency attenuates autoimmune disease in *Fas*<sup>lpr</sup> mice by modulating B cell activation and apoptosis**

**Yingying Luan, Qing Min, Runyun Zhang, Zichao Wen, Xin Meng, Ziyang Hu, Xiaoqian Feng, Meiping Yu, Lulu Dong, and Ji-Yang Wang**



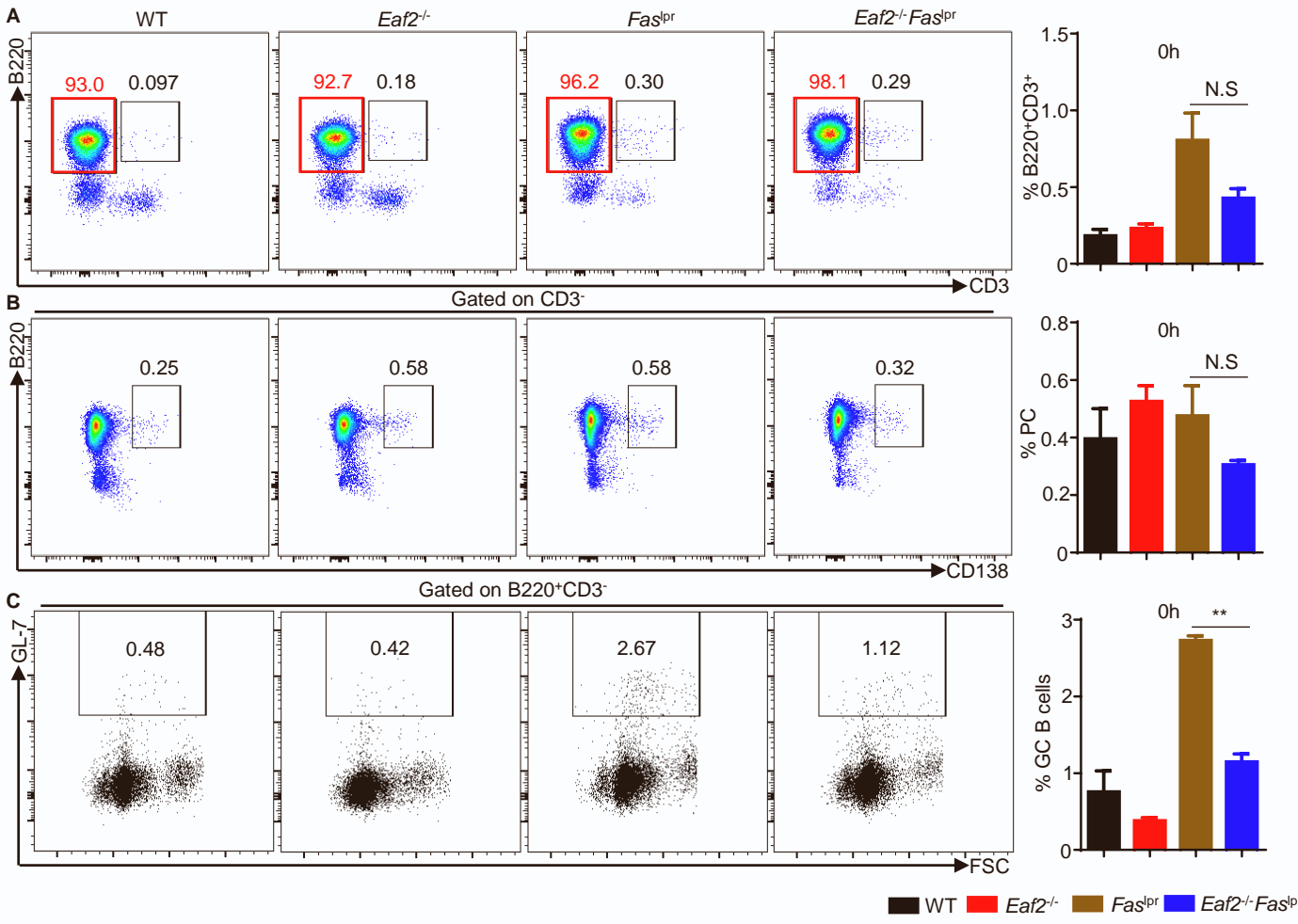
**Supplemental Figure 1. Genetic backgrounds of WT, *Eaf2*<sup>-/-</sup>, *Fas*<sup>pr</sup>, *Eaf2*<sup>-/-</sup>*Fas*<sup>pr</sup> female mice. Related to Figure 1. The backgrounds were determined using genomic single nucleotide polymorphism (SNP) testing (n ≥ 3). (A) Percentage of B6 and MRL genetic backgrounds in each mouse. (B) Average genetic background values for each genotype. (C) Statistical analysis of B6 and MRL genetic backgrounds across groups.**

## Supplemental Figure 2



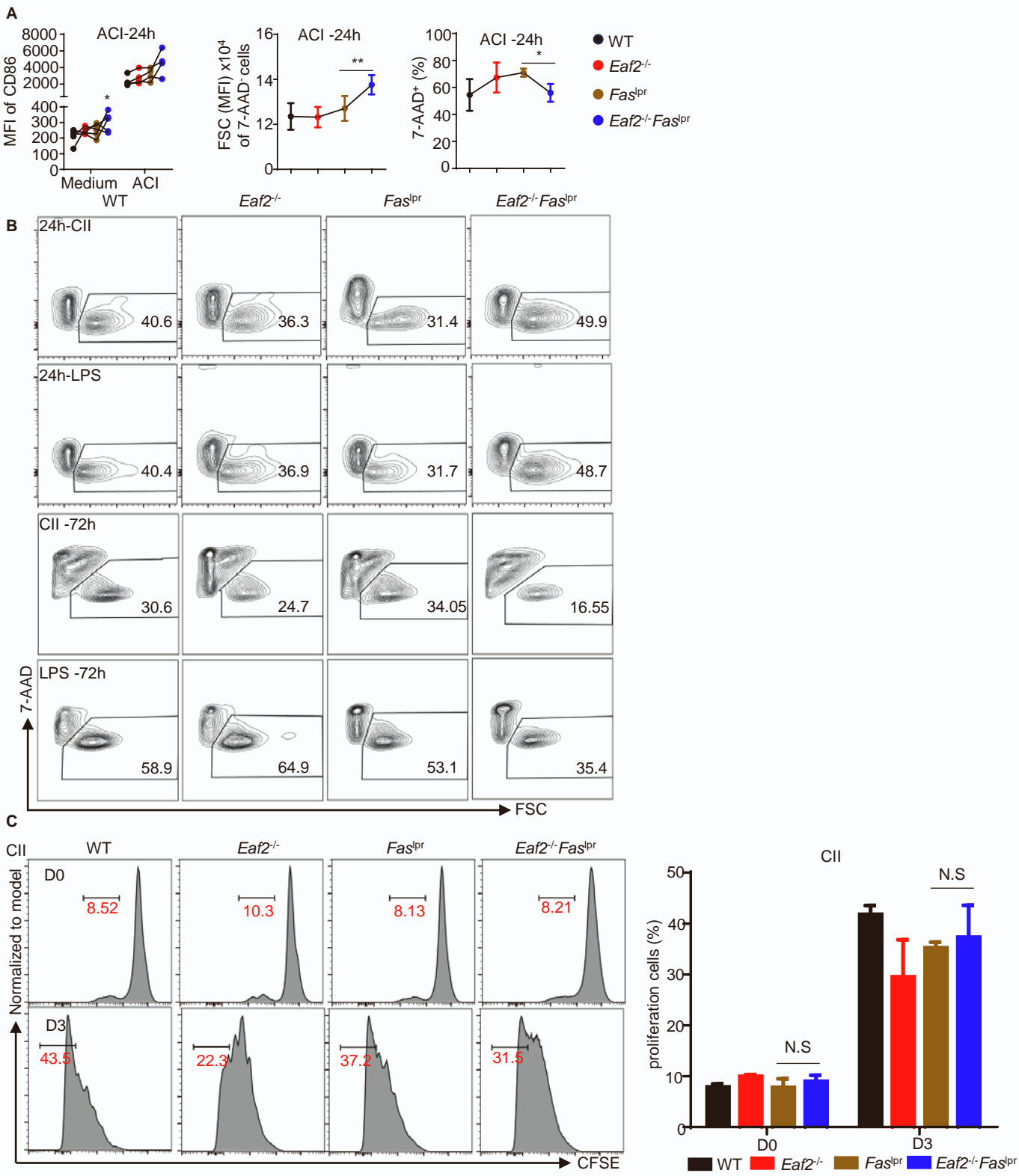
**Supplemental Figure 2. Impact of EAF2 deficiency on B cell development and maturation in *Fas*<sup>pr</sup> mice. Related to Figure 3.** Spleen cells from WT, *Eaf2*<sup>-/-</sup>, *Fas*<sup>pr</sup>, *Eaf2*<sup>-/-</sup> *Fas*<sup>pr</sup> female mice (aged 7-12 weeks, n ≥ 3) were stained and analyzed by flow cytometry for various B cell subsets. Representative flow cytometry plots show (A) B-1a (CD19<sup>+</sup>CD43<sup>+</sup>CD5<sup>+</sup>), B-1b (CD19<sup>+</sup>CD43<sup>+</sup>CD5<sup>-</sup>) and B-2 (CD19<sup>+</sup>CD43<sup>-</sup>CD5<sup>-</sup>) cells; (B) Total transitional B (CD19<sup>+</sup>B220<sup>+</sup>CD93<sup>+</sup>) cells; (C) T1 (B220<sup>+</sup>CD93<sup>+</sup>IgM<sup>+</sup>CD23<sup>-</sup>), T2 (B220<sup>+</sup>CD93<sup>+</sup>IgM<sup>+</sup>CD23<sup>+</sup>), and T3 (B220<sup>+</sup>CD93<sup>+</sup>IgM<sup>-</sup>CD23<sup>+</sup>) subsets; (D) MZ B (B220<sup>+</sup>CD21<sup>hi</sup>CD23<sup>lo</sup>) and FO B (B220<sup>+</sup>CD21<sup>+</sup>CD23<sup>+</sup>) cells. (E-L) Mean ± SEM of various B cell subsets from at least three independent experiments. Statistical significance was assessed by one-way ANOVA. \*p < 0.05; \*\*p < 0.01; \*\*\*p < 0.001.

**Supplemental Figure 3**



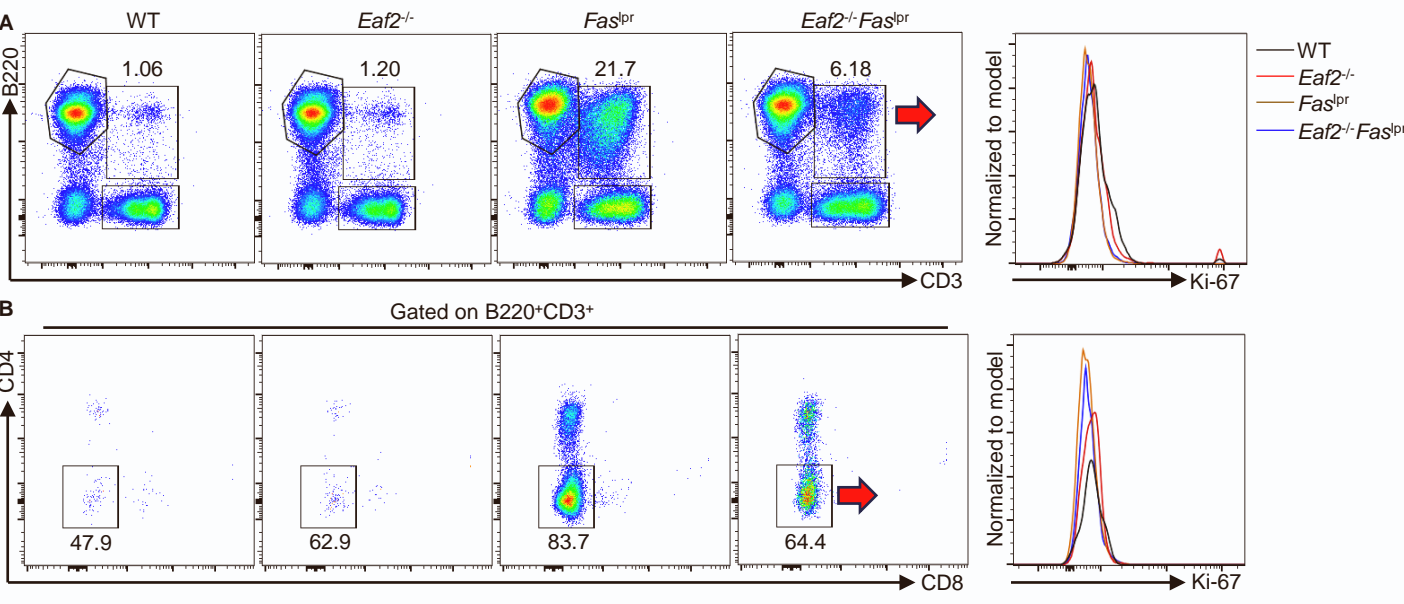
**Supplemental Figure 3. Phenotype of purified B cells. Related to Figure 4.** B cells from WT, *Eaf2*<sup>-/-</sup>, *Fas*<sup>lpr</sup>, *Eaf2*<sup>-/-</sup>*Fas*<sup>lpr</sup> female mice (7-12 weeks of age, n ≥ 3) were analyzed by flow cytometry for their (A) B220 and CD3, (B) B220 and CD138, and (C) FSC and GL-7 expression.

**Supplemental Figure 4**

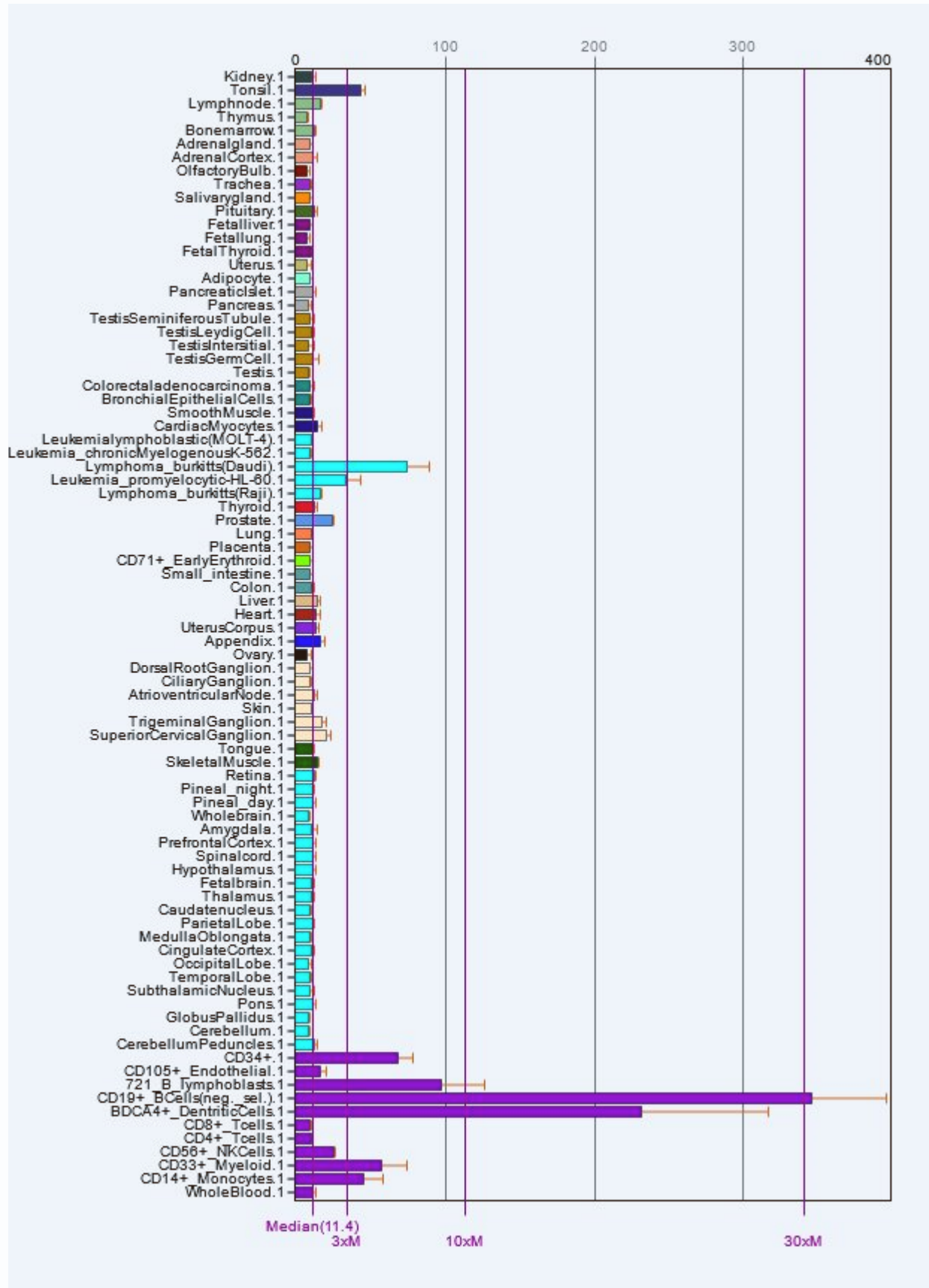


**Supplemental Figure 4. B cell activation, death and proliferation analysis. Related to Figure 4.** (A) B cells from WT, *Eaf2*<sup>-/-</sup>, *Fas*<sup>lpr</sup>, *Eaf2*<sup>-/-</sup> *Fas*<sup>lpr</sup> female mice (7-12 weeks of age, n ≥ 3) were stimulated with ACI for 24 h and analyzed for CD86 expression, FSC, and cell viability. (B) Representative flow cytometry of 7-AAD staining after CD40L+IL4+IL21 and LPS stimulation for 24 h and 72 h. (C) Purified spleen B cells were labeled with CFSE and stimulated with CII for 3 days. CFSE dilution was analyzed by flow cytometry. Left, representative flow cytometry profiles; right, summary of three independent experiments.

Supplemental Figure 5



**Supplemental Figure 5. Ki-67 expression in the abnormal B220<sup>+</sup>CD3<sup>+</sup> T and B220<sup>+</sup>CD3<sup>+</sup>CD4<sup>-</sup>CD8<sup>-</sup> (DN) T cells. Related to Figure 5.** Spleen cells from WT, *Eaf2*<sup>-/-</sup>, *Fas*<sup>lpr</sup>, *Eaf2*<sup>-/-</sup> *Fas*<sup>lpr</sup> female mice (7-12 weeks of age, n ≥ 3) were stained with anti-Ki-67 and analyzed for Ki-67 expression in gated B220<sup>+</sup>CD3<sup>+</sup> T (upper panels) and B220<sup>+</sup>CD3<sup>+</sup>CD4<sup>-</sup>CD8<sup>-</sup> (DN) T cells (lower panels). Left, gating strategy; right, overlay of Ki-67 expression.



Supplemental Figure 6. Expression of human *EAF2* in B cells and Burkitt's lymphomas. Related to Figure 6. Data sourced from BioGPS ([EAF2 \(ELL associated factor 2\) | Gene Report | BioGPS](#)).